

## Application of the Zone Melting Technique to Metal Chelate Systems. VII. Computer-assisted Consideration on the Solute Distribution Profiles in Zone Melting Process

Shigeru MAEDA, Hiroshi KOBAYASHI, and Keihei UENO

Department of Organic Synthesis, Faculty of Engineering, Kyushu University, Fukuoka 812

(Received February 1, 1973)

A new equation is derived which gives the solute distribution along a column after a zone melting chromatography (ZMC) process, where the initial charge of a sample mixture of  $k < 1$  is placed on the upper end of the column, one zone length high. The solute distribution differs significantly from that obtained by Pfann's equation on an infinite ingot, in the neighborhood of the upper end as expected from the difference in the initial conditions. The solute distribution is calculated numerically for the case in which the initial charge is placed by several zone lengths on the column top. The present multiple zone charge method shows little difference in solute distribution from the conventional single zone charge method, having the advantage of increasing the sample amount to be fractionated. Numerical calculation is performed to find the zone length with which the greatest amount of the solute of  $k < 1$  is concentrated into the bottom fraction of a certain length of a given column after each zone pass. A series of resulting zone lengths, showing a stepwise shortening, pass after pass, provides the optimum mode of decrease in the zone length.

We successfully applied the zone melting method to systems containing metal chelates.<sup>1-6</sup> The basic theory of zone melting was thoroughly covered by Pfann.<sup>7</sup> We have extended the theory by presenting mathematical expressions which give the solute distribution profile in specific methods of zone melting operation for a higher separation efficiency. Discussion is given on the theoretical basis for the experimental work. Since the equations are not given in simple analytical forms, the solute distribution profiles were computed numerically by use of FACOM 230—60 of the Computer Center of Kyushu University.

### Solute Distribution on a Semi-infinite Column in Zone Melting Chromatography (ZMC)

The basic equation determining the solute distribution along the solid column after  $n$ -th zone pass was described in the form of difference differential equation on the basis of mass balance as follows.<sup>8)</sup>

$$dC_n(x)/dx = k\{C_{n-1}(x+l) - C_n(x)\}/l \quad (1)$$

where  $l$  is the length of a molten zone,  $x$  denotes the position of the freezing interface of the zone which travels in the positive  $x$  direction,  $C_n(x)$  is the solute concentration at  $x$  after the  $n$ -th zone pass, and  $k$ , the distribution coefficient, is defined as a ratio of

solute concentration (weight/volume) in the frozen solid to that in the molten liquid.

Analytical solutions of Eq. (1) were derived by Reiss and Helfand<sup>9)</sup> for various types of ZMC methods on the following assumptions for simplification:

- 1) a constant distribution coefficient  $k$ , regardless of the concentration of the solute or freezing conditions,
- 2) no diffusion in the solid,
- 3) infinitely rapid mixing in the melt,
- 4) a negligibly small change in density upon freezing,
- 5) a constant zone length,  $l$ ,
- 6) flat solid-melt interfaces perpendicular to the column axis,
- 7) a uniform cross section of the column.

When the initial charge of a sample is placed at midpoint on an infinitely long column of a uniform unit cross section (Fig. 1), distribution of the solute is given by an analytical expression,<sup>8)</sup> which is further simplified by Pfann<sup>9)</sup> as

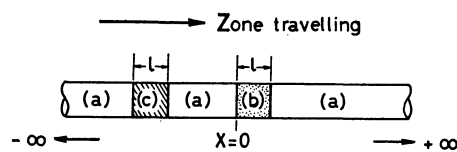


Fig. 1. ZMC on an infinitely long column  
(a): Pure solid solvent  
(b): Initial charge of sample mixture  
(c): Molten zone

$$C_n(x) = C_i k [k\{(x/l) + m\}]^m \exp[-k\{(x/l) + m\}]/m! \quad (2)$$

where  $m = n - 1$ ,  $-\infty < x < +\infty$ , and  $C_i$  is the concentration of a solute in the initial charge.<sup>10)</sup>

Practically it is much easier to place the initial charge of a solute mixture on either end than at the midpoint of a pure solid solvent column.

9) W. G. Pfann, *Anal. Chem.*, **36**, p. 2231 (1964).

10) According to Pfann, [Ref. 7, pp. 10, 30 and 59 and *J. Appl. Phys.*, **35**, 258 (1964)], Eq. (2) is valid without the third and fourth assumptions, if concentration is expressed in weight fraction or mole fraction,  $l$  defined as the length of solid that is melted to form the zone and  $k$  is an effective value consistent with the freezing conditions.

\* Contribution No. 287 from the Department of Organic Synthesis, Kyushu University. Presented in part before the International Congress on Analytical Chemistry, April 7, 1972 in Kyoto. Part VI by the same authors, Ref. 6.

1) K. Ueno, H. Kaneko, and Y. Watanabe, *Microchem. J.*, **10**, 244 (1966).

2) H. Kaneko and K. Ueno, *Talanta*, **13**, 1525 (1966).

3) H. Kaneko, H. Kobayashi, and K. Ueno, *ibid.*, **14**, 1403 (1967).

4) H. Kaneko, H. Kanagawa, H. Kobayashi, and K. Ueno, *ibid.*, **14**, 1411 (1967).

5) N. Fukuda, H. Kobayashi, and K. Ueno, *ibid.*, **18**, 807 (1971).

6) S. Maeda, H. Kobayashi, and K. Ueno, *ibid.*, **20**, 653 (1973).

7) W. G. Pfann, "Zone Melting," 2nd ed., John Wiley and Sons, Inc., New York, N. Y. (1966).

8) H. Reiss and E. Helfand, *J. Appl. Phys.*, **32**, 228 (1961).

Solutes with  $k$  less than unity move in the direction of zone travelling, and no ZMC column is required which extends in the opposite direction to that of the zone travelling from the position of the initial charge.

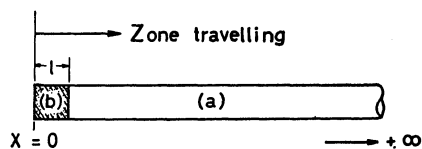


Fig. 2. ZMC on a semi-infinitely long column  
(a): Pure solid solvent  
(b): Initial charge of sample mixture and molten zone.

Assuming that the initial charge is placed one zone length high on the upper end of a semi-infinite column extending from  $x=0$  to  $x=+\infty$ , and that the zone travels downwards, Eq. (1) can be solved using iterative methods for each succeeding pass. After the first zone pass, it can be rewritten as

$$(l/k)\{dC_1(x)/dx\} + C_1(x) = C_0(x+l) \quad (3)$$

where  $C_0(x+l)=0$  regardless of  $x$  in the region  $x>0$ . Thus

$$dC_1(x)/C_1(x) = (-k/l)dx \quad (4)$$

A solution of this equation is

$$C_1(x) = C_1(0) \exp(-kx/l) \quad (5)$$

where  $C_1(0)=kC_0$

After the second zone pass, the basic differential equation is written as

$$(l/k)\{dC_2(x)/dx\} + C_2(x) = C_1(x+l) \quad (6)$$

The right hand side of this equation is given by Eq. (5), and we have

$$dC_2(x)/dx + (k/l)C_2(x) = (k/l)C_1(0) \exp\{-k(x+l)/l\} \quad (7)$$

A solution of this equation is analytically derived as

$$C_2(x) = \exp(-kx/l)\{C_2(0) + (kx/l)C_1(0)\exp(-k)\} \quad (8)$$

where

$$C_2(0) = (k/l) \int_0^l C_1(x)dx \quad (9)$$

Repeating similar treatments, after the  $n$ -th zone pass we have the following solution.

$$C_n(x) = \exp(-kx/l) \left\{ \sum_{r=0}^{n-1} (k/l)^r C_{n-r}(0) \times \exp(-rk)x(x+r)^{r-1}/r! \right\} \quad (10)$$

where

$$\begin{aligned} C_n(0) &= (k/l) \int_0^l C_{n-1}(x)dx \\ &= \{1 - \exp(-k)\}C_{n-1}(0) + \sum_{r=1}^{n-2} C_{n-1-r}(0) \exp(-rk) \\ &\quad \times \left[ \{1 - \exp(-k)\} + (k/l)^r \sum_{p=0}^{r-1} \frac{l^p(r-l)^{r-p-1} - l(p+1)\exp(-k)\{(r+1)l\}^{r-p-1}}{(k/l)^p(r-p)!} \right] \end{aligned} \quad (11)$$

Equation (10) can be readily proved to be one of the analytical solutions of Eq. (1) by the method of mathematical induction (Appendix).

Equations (10) and (11) are highly iterative and can be calculated only by a digital computer for relatively large  $n$ -values, the results being illustrated in Fig. 3 along with those of Eq. (2) for comparison. Solute distribution by Eq. (10) differs from that by Eq. (2) with respect to the fact that the solute does not distribute in the region of negative  $x$ , namely

$$\int_0^{+\infty} C_n(x)dx = 1$$

for Eq. (10) in contrast to

$$\int_{-\infty}^{+\infty} C_n(x)dx = 1$$

for Eq. (2).

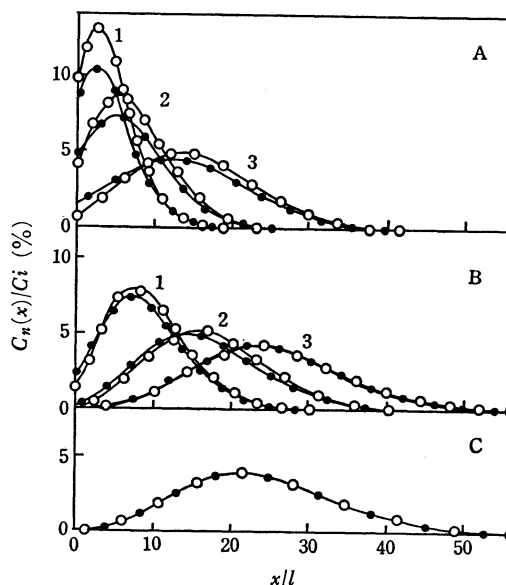


Fig. 3. Comparisons of the distribution profiles between Reiss-Helfand's and the present equations.  
○—○ the present equation (10)  
●—● Reiss-Helfand's equation (2)  
A:  $k=0.80$ , 1;  $n=10$ , 2;  $n=20$ , 3,  $n=50$   
B:  $k=0.56$ , 1;  $n=10$ , 2;  $n=20$ , 3;  $n=30$   
C:  $k=0.30$ ,  $n=10$ .

A comparison of curves from both equations indicates that the distribution curves of Eq. (10) shift to the direction of positive  $x$  slightly greater than those of Eq. (2), obviously owing to the effect of a semi-infinite column as mentioned above. This tendency is especially marked when the solute distribution peak is in the neighborhood of the column top. Otherwise, the distribution curves from Eq. (10) are almost superimposable on those from Eq. (2).

If we refer to Eq. (2), the peak position  $x_{\max}$  increases linearly with  $n$ , as is given by

$$x_{\max}/l = (n-1)(1-k)/k \quad (12)$$

On the other hand, if we refer to Eq. (10), it is difficult to obtain such a relationship mathematically. Numerical calculation affords the relationship between  $x_{\max}/l$  and  $n$ , which is slightly deviated from linearity in the range of small  $n$ -values (Fig. 4),  $x_{\max}/l$  being generalized dimensionless expression of the peak position.

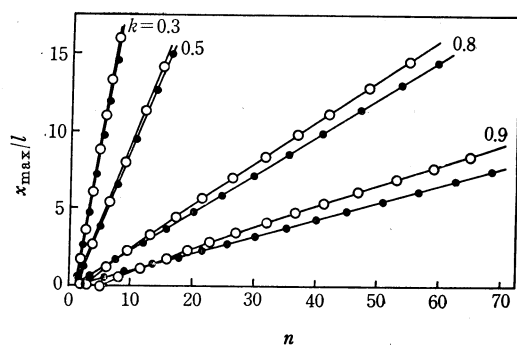


Fig. 4. The peak position versus number of zone passes.

- The present equation (10)  
●—● Reiss-Helfand's equation (2)

### ZMC Distribution Curve on a Multiple Zone Charge Method

The theory of ZMC fractionation tells us that the separation between two components having different  $k$ -values becomes more effective with increasing number of zone passes  $n$ , as shown by Eq. (12),<sup>9</sup> the shorter zone length being required for attaining the more efficient separation on the column of a limited length,  $L$ . However, such shortened zone length would decrease the amount of the sample to be fractionated, as long as the sample mixture was placed initially one zone length high. Thus the question arises of how the separation is affected when the initial charge of a sample mixture is placed by more than single zone length on the column top.

Assuming that the sample mixture of  $k$  less than unity is charged by  $T$ -folds of a unit zone length  $l$  on the upper end of a column from which a zone starts to travel downwards (Fig. 5), the solute distribution after a ZMC process can be calculated as follows.

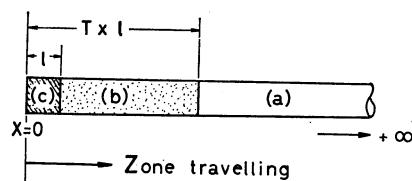


Fig. 5. Multiple zone charge method.  
(a): Pure solid solvent  
(b): Initial charge of sample mixture  
(c): Molten zone

At the first zone pass, in so far as the freezing interface of a molten zone moves in the region  $0 < x < (T-1)l$ , the solute is distributed by an ordinary zone melting process according to the equation,<sup>7)</sup>

$$C_1(x)/C_i = 1 - (1-k) \exp(-kx/l) \quad (13)$$

where  $0 < x < (T-1)l$ .

When the freezing interface arrives at  $x = (T-1)l$ , the solute concentration in the solid just frozen at this point is given by

$$C_1(x)/C_i = 1 - (1-k) \exp\{-k(T-1)\} \quad (14)$$

The solute concentration in the molten zone is therefore given by

$$C_i' = C_i [1 - (1-k) \exp\{-k(T-1)\}] / k \quad (15)$$

From this point, ZMC process begins with  $C_i'$  as the initial concentration according to an equation analogous to Eq. (5):

$$C_1\{x - (T-1)l\} = kC_i' \exp[-k\{x - (T-1)l\}/l] \quad (16)$$

After the second zone pass, the solute is redistributed according to Eq. (1) from the solute distribution profile developed on the preceding zone pass. The analytical method for determining the solute distribution profile is generally too complicated, and a numerical computation provides much easier solution.

Computation was carried out by the Runge-Kutta-Gill method for Eq. (1), taking the zone length  $l$  and the initial concentration  $C_i$  both as unity, the grid spacing being one twentieth of the zone length.<sup>11)</sup> The solute concentration at the upper end of the column on each pass  $C_n(0)$  is given by

$$C_n(0) = k \int_0^1 C_{n-1}(x) dx \quad (17)$$

which was also computed by use of Simpson's numerical integration method with an integration step equal to the grid spacing.

Numerically computed concentration profile after each pass was counter-checked by Simpson's integration of a solute amount over the whole range of solute distribution in a similar procedure to that described above. The integrated magnitude of the solute amount remained constant from pass to pass, being equal to that in the initial charge  $TC_i$ .

A few examples of solute distribution profiles after 20 zone passes are shown in Fig. 6. Each curve is normalized for comparison, which suggests that there are very little differences between the distribution curves where  $T$ -values are less than 5, especially in the case of small  $k$ -values. The situation is further clarified by Figs. 7 and 8 showing the peak position and the half peak width plotted against  $n$  for a certain range of  $T$ -values, respectively, which were also numerically computed. If one compares the peak position of the multiple zone charge method with that of the ordinary single zone charge method ( $T=1$ ) in the case of  $k=0.3$  after 40 zone passes, the peak position by the former method shifts towards positive  $x$  only 1.3% of that by the latter method. Even in the case of  $k=0.8$ , the relative distance of the shift is within 8%. Fig. 8 indicates that the difference in the half peak widths between the two methods is also insignificant; the relative differences are within only 0.4 and 3.5% for

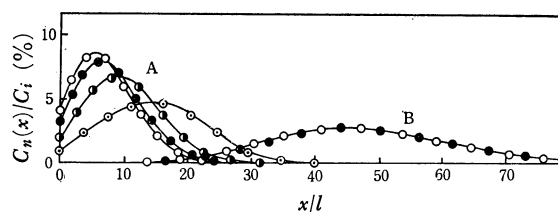


Fig. 6. Solute distribution curves by multiple zone charge method after 20th zone pass, where  $T$  means multiplicity of multiple zone charge.  
○  $T=1$ , ●  $T=5$ , ◐  $T=10$ , ⊙  $T=20$   
A:  $k=0.8$ , B:  $k=0.3$

11) L. Lapidus, "Digital Computation for Chemical Engineers," McGraw-Hill, Inc., New York, N. Y. (1962), p. 89.

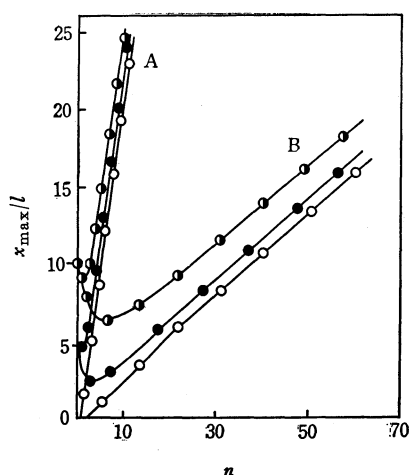


Fig. 7. Peak position of multiple zone charge sample.  
 ○  $T=1$ , ●  $T=5$ , ◐  $T=10$   
 A:  $k=0.3$ , B:  $k=0.8$

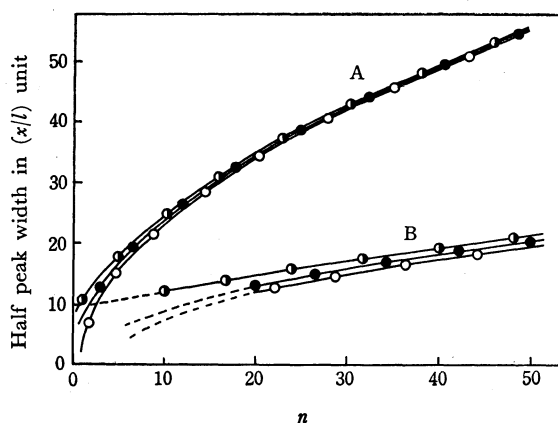


Fig. 8. Half peak width of distribution profiles versus number of zone passes.  
 ○  $T=1$ , ●  $T=5$ , ◐  $T=10$   
 A:  $k=0.3$ , B:  $k=0.8$

$k=0.3$  and  $0.8$  after 40 zone passes, respectively, the difference decreasing considerably with increase in number of zone passes. As far as the efficacy as a separating method is concerned, we could find no disadvantages in the present multiple zone charge method as compared with the ordinary single zone charge method.

This method should be useful working with a large quantity of sample or solutes, solubilities of which in a solid solvent are relatively small. With use of the single zone charge method, even if the length of the initial charge is not rigorously equal to a unit zone length, no significant difference would result as regards the solute distribution profile.

### An Optimum Mode of Stepwise Decreasing Zone Length for Improving the Concentrating Efficiency by Zone Melting Method

Regarding the efficiency of the zone melting method as a separating technique, normal freezing was the most effective at the first zone pass and the shorter zone length was the more effective after an indefinitely

large number of zone passes,<sup>12)</sup> and the solute concentration profile is expected to approach very rapidly the ultimate distribution by adjusting the zone length in the following manner; at the first zone pass,  $l=L$ , namely normal freezing process, and after the second pass, zone length decreases stepwise pass after pass. Such a method would be useful from the viewpoint of saving time.

Eckslager and co-workers calculated the efficiency as a refining method for the cases where zone length decreased in seemingly arbitrary manner with increase in zone passes.<sup>13)</sup> We have also investigated the technique, and calculated the optimum mode of stepwise decrease of zone length, which gave the maximum concentration in the bottom portion of a given length  $S$  after each zone pass.

Optimization of zone length is carried out in the following procedure for a set of specified  $k$ - and  $S$  values: 1) At the first zone pass ( $n=1$ ), zone length is equal to the total column length  $L$ , the solute distribution being therefore determined by the normal freezing process, which has been given analytically<sup>14)</sup> as

$$C_1(x) = kC_0(1-x/L)^{k-1} \quad (18)$$

where  $x$  denotes the position of the freezing interface as  $x=0$  at the column top, and  $C_0$  the initial concentration of a solute of  $k$  less than unity in the ingot.

2) At the second pass ( $n=2$ ), based upon the distribution profile developed by the normal freezing process, distribution profiles are numerically calculated for 200 different zone lengths  $l_j$  with an increment of  $0.005L$  unit from  $0.005L$  to  $1.0L$ .

$$l_j = 0.005Lj \quad j = 1, \dots, 200 \quad (19)$$

Computation for the region of the zone melting process was programmed by the Runge-Kutta-Gill method for Eq. (1)<sup>11)</sup>, where  $n=2$  and  $l=l_j$  ( $j=1, \dots, 200$ ), taking  $L=100$  and  $C_0=1$ , and grid spacing defined as  $L/2000$ . Normal freezing on the last zone length of the column is calculated numerically for the points in the region in  $L-l_j < x < L$  with an increment of  $L/2000$ , which is equal in magnitude to the grid spacing, according to the analytical equation

$$C_{nj}(x) = kC'_j\{(L-x)/l_j\}^{k-1} \quad (20)$$

where

$$C'_j = C_{nj}(L-l_j)/k \quad (21)$$

$n=2$  and  $L-l_j < x < L$ .

Solute concentration at the column top,  $C_{2j}(0)$ , is given by

$$C_{2j}(0) = k \int_0^{l_j} C_1(x) dx \quad (22)$$

This was computed by Simpson's numerical method with an integration step equal to the grid spacing defined in the Runge-Kutta-Gill calculation.

Solute amount in the bottom portion of a specified length  $S$  is given by

12) a) L. Burris, Jr., C. H. Stockman, and I. G. Dillon, *Trans. AIME*, **203**, 1017 (1955). b) W. G. Pfann, Ref. 7, pp. 31 and 42-45.

13) K. Eckslager, V. Ettel, P. Stopka, and Z. Kodejs, *Coll. Czech. Chem. Commun.*, **36**, 3900 (1971).

14) W. G. Pfann, Ref. 7, p. 11.

$$M_{nsj} = G_0 L - \int_0^{L-S} G_{nj}(x) dx \quad (23)$$

where  $n=2$ , assuming a unit cross section of the column. The second term for each distribution profile was computed also by Simpson's method in a similar manner to that described above.

The distribution profile giving the highest value of  $M_{2sj}$  with different  $j$  is then stored into the memory for calculation of zone lengths in the 3rd pass, and the zone length bringing the highest  $M_{2sj}$ -value is defined as the optimum zone length in the 2nd pass.

3) At the  $n$ -th pass after the third pass, the optimum zone length is determined in a similar manner to that described above, from the distribution profile which is brought by the optimized  $(n-1)$ -th zone pass. The distribution profile which is formed by the zone length

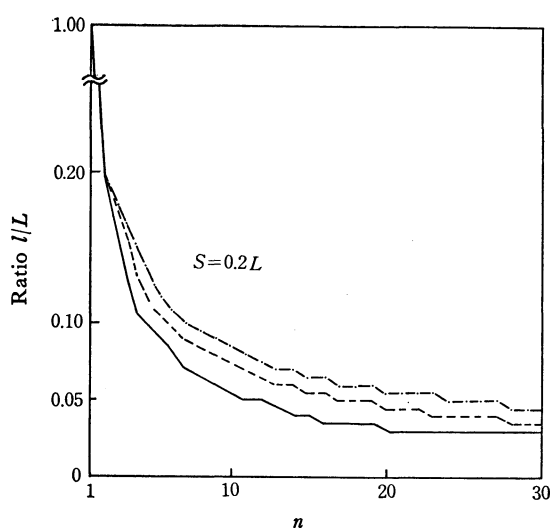


Fig. 9—1. Optimum zone length in ratio to  $L$  on each zone pass.

---  $k=0.8$ , ---  $k=0.5$ , —  $k=0.2$

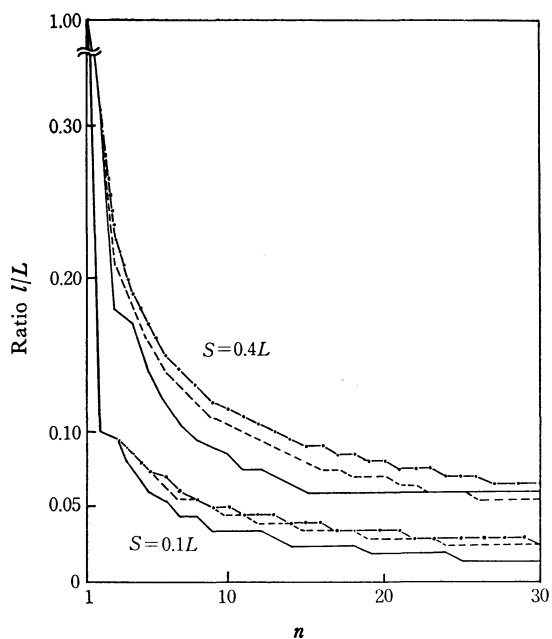


Fig. 9—2. Optimum zone length in ratio to  $L$  on each zone pass.

---  $k=0.8$ , ---  $k=0.5$ , —  $k=0.2$

optimized for the  $n$ -th pass, is then stored for computation of the zone lengths in the  $(n+1)$ -th pass.

Fig. 9 shows a few examples of the optimized mode of stepwise decrease of zone length for various  $k$  and  $S$ -values.

The superior efficacy of the present decreasing zone length (DZ) method is shown in Fig. 10 and Tables 1 and 2, in comparison with the conventional constant zone length (CZ) method.

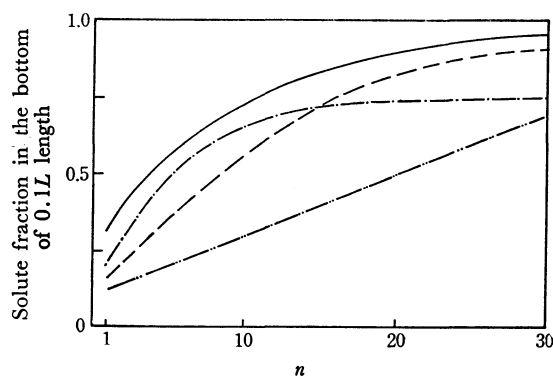


Fig. 10. Solute fraction concentrated into the bottom portion of  $0.1L$  length after  $n$ -th zone pass,  $k=0.5$ .

— DZ method, --- CZ method,  $l=0.05L$ , -.- CZ method,  $l=0.10L$ , -.-.- CZ method,  $l=0.02L$

In Fig. 10 the solute fraction, which is concentrated in the bottom portion of  $S=0.1L$ , is plotted against number of zone passes upon applying the DZ- and CZ methods to a system of  $k=0.5$ . It is apparent that, though the solute is concentrated in various ways to the bottom portion, efficiency in concentrating a solute by the DZ method is always superior to the CZ method, when compared at the same number of zone passes.

TABLE 1. FRACTION CONCENTRATED INTO A PORTION OF  $0.1L$  AT THE BOTTOM AFTER THE 30TH ZONE PASS

$k$	DZ method	CZ method		
		$l=0.1L$	$l=0.05L$	$l=0.02L$
0.1	1.0000	0.9899	0.9997	1.0000
0.2	1.0000	0.9599	0.9970	1.0000
0.3	0.9997	0.9099	0.9883	0.9906
0.4	0.9955	0.8399	0.9663	0.8915
0.5	0.9600	0.7491	0.9077	0.6883
0.6	0.8435	0.6337	0.7716	0.4977
0.7	0.6388	0.4911	0.5661	0.3535
0.8	0.4081	0.3355	0.3584	0.2445
0.9	0.2195	0.1976	0.2000	0.1614

Table 1 gives a comparison of the two methods as regards concentrating techniques. Values indicate the fraction of the solute concentrated into the bottom portion of  $0.1L$  after 30 zone passes.

Table 2 gives a comparison from a viewpoint of refining efficiency. Values indicate the length (% to  $L$ ) of the portion which is purified to the average concentration level indicated on each heading. After 30 zone passes of the DZ method, for example, within 79.7% of the column length from the top, averaged

TABLE 2. LENGTH OF PURIFIED PORTION IN % OF A WHOLE LENGTH FROM THE COLUMN TOP AFTER THE 30 TH ZONE PASS

$C_{av}/C_0$	DZ method		CZ method					
			$l=0.1L$		$l=0.05L$		$l=0.02L$	
	1/100	1/1000	1/100	1/1000	1/100	1/1000	1/100	1/1000
$k=0.1$	97.9	96.5	89.7	82.3	94.9	91.2	97.9	96.5
0.2	96.8	95.1	83.6	74.6	91.9	87.6	96.8	95.0
0.3	95.7	93.1	77.9	65.9	89.3	83.5	89.4	62.7
0.4	91.8	81.7	70.5	54.6	85.3	72.3	49.5	29.9
0.5	79.7	48.7	59.3	32.3	62.7	24.2	25.1	9.6
0.6	43.4	2.2	31.2	0	20.2	0	8.1	0
0.7	0	0	0	0	0	0	0	0
0.8	0	0	0	0	0	0	0	0
0.9	0	0	0	0	0	0	0	0

concentration  $C_{av}$  of an impurity of  $k=0.5$  is less than 1/100 of the initial concentration  $C_0$ , and within 48.7 % of the column length, the impurity level is less than 1/1000, while by the CZ method of  $l=0.02L$ , the corresponding length is 25.1 and 9.6% for the respective impurity levels.

It should be mentioned that, since a series of the optimum zone lengths is determined by a specified set of  $k$ - and  $S$  values of a system under consideration, and since the mode of stepwise decrease of zone length differs considerably with  $k$ - and  $S$  values, difficulties remain in the instrumentation of the present DZ method.

### Appendix

Proof that Eq. (10) is a solution of Eq. (1).

If  $K_n(x)$  is defined by

$$K_n(x) = \exp(\beta x) C_n(x) \quad (24)$$

where  $\beta=k/l$ , then Eqs. (1) and (10) can be rewritten respectively as

$$dK_n(x)/dx = \beta \exp(-k) K_{n-1}(x+l) \quad (25)$$

$$K_n(x) = \sum_{r=0}^{n-1} \beta^r C_{n-r}(0) \exp(-rk) x(x+rl)^{r-1}/r! \quad (26)$$

Equation (10) can be verified to be a solution of Eq. (1) by showing that Eq. (26) is a solution of Eq. (25).

First, we verify that Eq. (26) is a solution of Eq. (25) when  $n=1$ .

From Eq. (26),  $K_1(x)$  is given by

$$K_1(x) = C_1(0) \quad (27)$$

By substituting Eq. (5) into Eq. (24) where  $n=1$ , Eq. (27) can be found to hold under the present initial conditions.

Assuming that Eq. (26) is the right solution at  $n=N$ , we verify that it also holds for  $n=N+1$ .

Equation (25) is written for  $n=N+1$  as

$$dK_{N+1}(x)/dx = \beta \exp(-k) K_N(x+l) \quad (28)$$

By integrating the equation over the region from 0 to  $x$ , we have

$$\int_0^x dK_{N+1}(x) = \beta \exp(-k) \int_0^x K_N(x+l) dx \quad (29)$$

or

$$K_{N+1}(x) - K_{N+1}(0) = \beta \exp(-k) \int_0^x K_N(x+l) dx \quad (30)$$

By substituting Eq. (26) into Eq. (30), the right-hand side is written as

$$\begin{aligned} & \beta \exp(-k) \int_0^x K_N(x+l) dx \\ &= \beta \exp(-k) \sum_{r=0}^{N-1} [\beta^r C_{N-r}(0) \exp(-rk)/r!] \\ & \times \int_0^x (x+l) \{x+(r+1)l\}^{r-1} dx \end{aligned} \quad (31)$$

The last integration can be readily performed to give

$$\int_0^x (x+l) \{x+(r+1)l\}^{r-1} dx = x \{x+(r+1)l\}^r / (r+1)$$

Substituting this relation into Eq. (31), we obtain

$$\begin{aligned} & \beta \exp(-k) \int_0^x K_N(x+l) dx \\ &= \beta \exp(-k) \sum_{r=0}^{N-1} \beta^r C_{N-r}(0) \\ & \times \exp(-rk) x \{x+(r+1)l\}^r / (r+1) \\ &= \sum_{r=0}^{N-1} \beta^{(r+1)} C_{N-r}(0) \\ & \times \exp\{-(r+1)k\} x \{x+(r+1)l\}^r / (r+1)! \end{aligned} \quad (32)$$

Substituting this relation into Eq. (30), and considering the identity

$$K_{N+1}(0) = C_{N+1}(0) \quad (33)$$

which is readily derived from Eq. (24), we have

$$\begin{aligned} K_{N+1}(x) &= C_{N+1}(0) + \sum_{r=0}^{N-1} \beta^{(r+1)} C_{N-r}(0) \\ & \times \exp\{-(r+1)k\} x \{x+(r+1)l\}^r / (r+1)! \\ &= \sum_{s=0}^N \beta^s C_{N+1-s}(0) \exp(-sk) x(x+sl)^{s-1}/s! \end{aligned} \quad (34)$$

where  $s=r+1$ .

This can readily be seen to be equivalent to Eq. (26), where  $n=N+1$ . Equation (26) is proved by mathematical induction to be a solution of Eq. (25) for all  $n$ ,  $n$  being any positive integer. Thus by introducing Eq. (26) into Eq. (24), we obtain Eq. (10).

The authors are grateful to Dr. S. Gondo, Department of Chemical Engineering, and Mr. T. Tsuneyuki, Department of Organic Synthesis, Kyushu University, for their helpful advice in FORTRAN programming.